SUPPLEMENTAL MATERIAL

Fibulin-4 deficiency results in ascending aortic aneurysms: a potential link between abnormal smooth muscle cell phenotype and aneurysm progression

Jianbin Huang, Ph.D., Elaine C. Davis, Ph.D., Shelby L. Chapman, Madhusudhan Budatha, Ph.D., Lihua Y. Marmorstein, Ph.D., R. Ann Word, M.D. and Hiromi Yanagisawa, M.D., Ph.D.

Detailed Methods

Mouse

Conventional *Fbln4*$^{+/-}$ and *Eln*$^{+/-}$ mice were described previously [1, 2]. SM22-Cre transgenic mice were purchased from Jackson Laboratory, and CAG-Cre and Tie2-Cre transgenic mice were previously described [3, 4]. Wild-type littermates were used as controls for *Fbln4*^{GKO} embryos. *Fbln4*$^{loxP/+}$ or *Fbln4*$^{KO/+}$ littermates, carrying the same copy number of Cre-transgene as mutants were used as controls for *Fbln4*^{SMKO} or *Fbln4*^{ECKO} mice. All animal protocols were approved by the IACUC of the University of Texas Southwestern Medical Center.

Gene targeting and genotyping.

A *Fbln4*-targeting vector was generated using the pGKNEO-F2L2-DTA vector containing a neomycin resistance cassette flanked by frt and loxP sites and a diphteria toxin (DTA) gene cassette. The arms contained approximately 9 kb of homologous regions, which were generated by high fidelity PCR amplification of 129SvEv genomic DNA (Expanded High Fidelity PCR System; Roche). The vector DNA was linealized with ScaI and electroporated into SM-1 ES cells as previously described [5]. After positive and negative selection with G418 (250 μg/ml) and DTA, 480 clones were subjected to PCR screening. Correct recombination was confirmed in 4 ES cell clones by Southern blot analysis using SacI-digested genomic DNA hybridized with a 5' probe and XbaI-digested DNA with a 3' probe. Four ES cell clones were expanded and injected into blastocysts obtained from C57BL/6 females. Chimeras derived from all four independent ES cell lines gave germ line transmission and heterozygous mice were mated with the FLPe deleter [6] to obtain a heterozygote for a conditional allele (*Fbln4*$^{loxP/+}$), or with CAG-Cre deleter to obtain a heterozygote for a null allele in germ cells (*Fbln4*$^{GKO/+}$). Subsequent genotyping was performed by PCR to detect a wild-type allele and loxP-containing allele (forward 5'-CTGCCCCTTCAAGAAGCTGG-3', reverse 5'-CCGGGATGGTCAGGCACTCG-3'), and null allele (forward 5'-CTTAGAGGGCCAGGGAGGTGAAGAC-3', reverse 5'-CCCTGCCTCTACCTTTGCCCAAGAG-3'), which yielded PCR products of 470kb, 670kb and 540kb, respectively.

Histology and immunohistochemistry.

For preparation of embryo sections, aortae and torsos were harvested en bloc and fixed in 4% paraformaldehyde, embedded in paraffin and 5-μm sections were prepared. For cryosections, tissues were embedded in OCT and frozen in liquid N_2, and 8-μm sections were prepared. Hematoxylin &Eosin (HE) staining was performed for routine histology and Masson-Trichrome and Hart's staining for detection of collagen fibers and elastic fibers, respectively. PAS and Alcian blue staining was performed for detection of accumulation of glycoproteins and mucopolysaccharides, respectively. Immunohistochemistry was performed as previously described [7] and antibodies are listed in Supplemental Table 1. Immunostaining and TdT-mediated dUTP nick end labeling (TUNEL) was performed according to the manufacturer's instructions (Roche). Sections were incubated with 4,6-diamidino-2-phenylindole (DAPI) (Vector laboratories) for visualization of all cellular nuclei. Three animals per genotype were used in analyses unless otherwise noted.

Electron microscopy.
Aortae were dissected from embryos following cardiac perfusion with 3% glutaraldehyde in 0.1M sodium cacodylate and samples were prepared as previously described [8]. Sections were viewed using a Tecnai 12 transmission electron microscope at 120 kV and images were digitally captured.

Western blot analysis.
Aortae were minced in 2x lammelli buffer and boiled at 95ºC for 10 min, and subjected to SDS-PAGE. Proteins were then transferred to a Western PVDF membrane (Millipore, Inc.) and immunoblotted with primary antibodies. Antibody information is provided in Supplemental Table 1. Membranes were then incubated with respective anti-mouse or anti-rabbit HRP-conjugated secondary antibody (1:3000, Bio-Rad) and visualized with chemoluminescence kit (Santa Cruz Biotechnology, Inc.). For E18.5 aorta extracts, 2 aortae were pooled and subjected to Western blot analysis. The experiments were performed two to three times using total of four to six embryos per genotype. For adult animals, individual aorta was harvested and subjected to Western blot analysis. The experiments were performed at least three times using a different sibling pairs of animals.

Gelatin Zymography
Descending thoracic aortae were pulverized in liquid N_2 and extracted in 50 mM Tris-HCl(7.5), 150 mM NaCl, 10 mM $CaCl_2$ and 0.1% (wt/vol) Triton X-100 at 4°C. The homogenates were centrifuged and total protein concentration was determined by Bradford assay (Bio-Rad). The aortic extracts (10 μg) were resolved by nonreducing 10% SDS-PAGE through gels containing 1 mg/ml gelatin. Gels were washed with 2.5 % Triton X-100 for 1 hr to remove the SDS, then incubated overnight (37°C) in 50 mM Tris-HCl, pH 8.0 and 5 mM $CaCl_2$. Zones of gelatinolytic activity were visualized after staining the gels with 0.5% Coomassie blue R-250.

Isolation of vascular smooth muscle cells and immunostaining.
Primary SMCs were isolated from explants of aortae harvested from E17.5-E18.5 wild-type and *Fbln4*^{GKO} aortae as described previously [9] and cultured in DMEM media containing 20% FBS, 100 U/ml penicillin and 100 U/ml streptomycin. SMCs were characterized by positive staining for SM α-actin (Sigma) and negative staining for CD31 (Pharmingen). Experiments were conducted using two independent preparations of SMCs from aortae derived from 4-6 wild-type or *Fbln4*^{GKO} embryos and SMCs were used under passage number 12.

Proliferation assays.
SMCs were plated at a density of 2 x 10^4 cells/well in 96-well dishes in serum containing media and were cultured for 24h, then serum-starved for 48 h followed by stimulation with 20% FBS for 4h. Cell numbers were quantified using Cell Titer 96 aqueous One solution (Promega) according to manufacture's instructions. For detection of cells in mitosis in serum-free condition, cells were plated in a 6-well plate at a density of 5 x 10^5 cells/well and incubated for 24 h before subjected to immunostaining with anti-phophorylated histone H3 (PH3).

Quantitative PCR.
RNA was isolated from aortae using a RNeasy Plus Micro Kit (QIAGEN) and 1μg of total RNA subjected to reverse transcription reactions using superscript III reverse transcriptase (Invitrogen). For preparation of E18.5 aorta RNA, three aortae were pooled together in each experiment unless noted otherwise. SYBR Green was used for amplicon detection and gene expression was normalized to expression of the housekeeping gene β2-microglobulin (β2M). PCR reactions were carried out in triplicates in a ABI Prism 7000 sequence detection system (Applied Biosystems) with one cycle of 3 min at 95°C, then 40 cycles of 10 sec at 95°C and 1 min at 55°C or in the CFX96 real-time PCR detection system (Bio-Rad) with one cycle of 3 min at 95°C, then 40 cycles of 10 sec at 95°C and 1 min at 60°C.

Levels of mRNA were determined using the ddCt method (Applied Biosystems) and expressed relative to the mean dCt of WT controls. In some experiments, sibling pairs were used and each mutant tissue was expressed relative to that of WT. Primer sequences are provided in Supplemental Table 2.

Antibody production
Rabbit polyclonal antibody BSYN5125 was raised against mouse fibulin-4 polypeptides (NH2-GCIVNNEHPQQETPAAEASS-OH; Biosynthesis Inc, Lewisville, TX).

Statistical analysis.
Student *t*- test or one-way ANOVA with the Bonferroni post hoc test was used for statistical analysis. $P < 0.05$ was considered statistically significant.

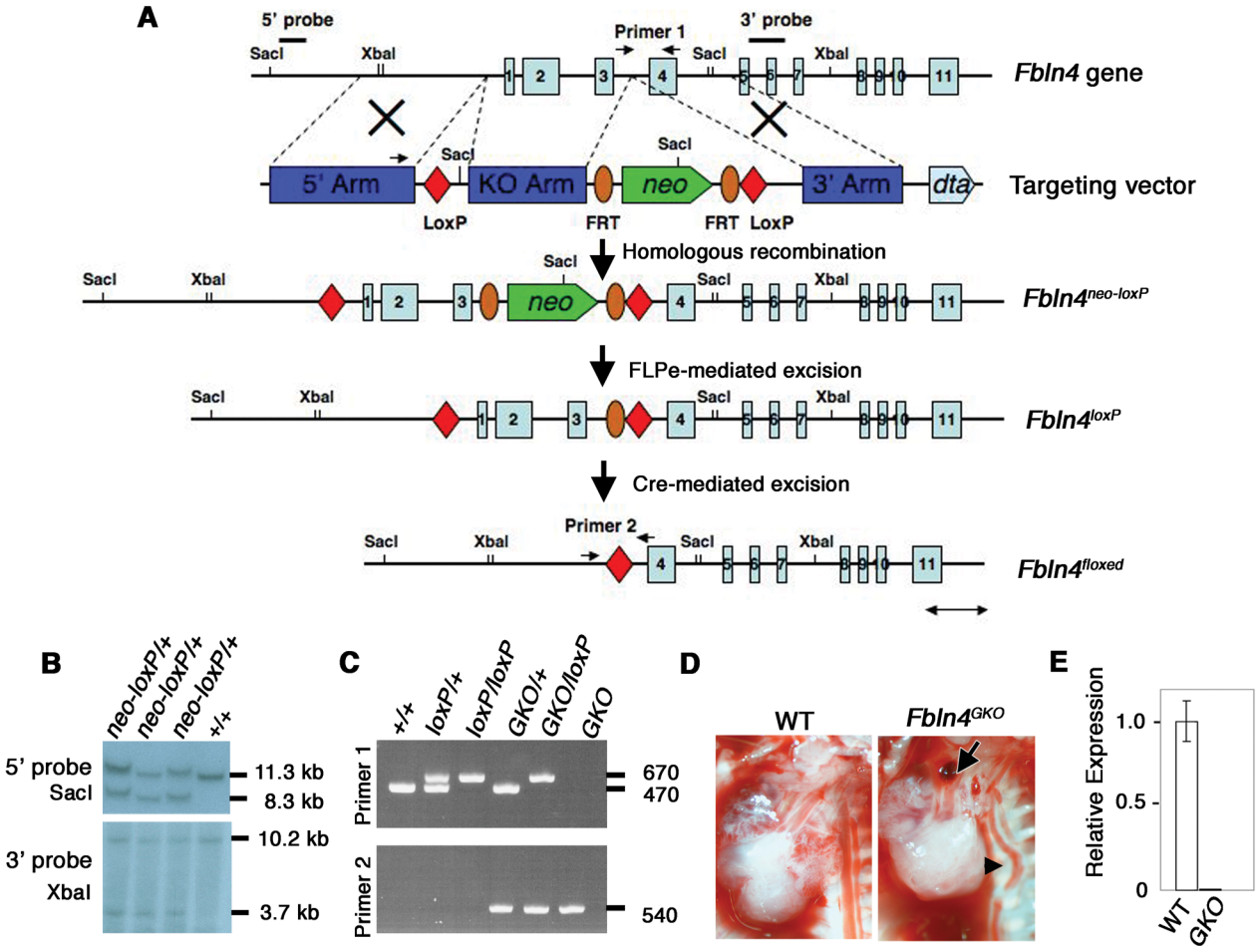

Online Figure I. Generation of *Fbln4* conditional knockout mice. **A.** Targeting strategy. Exons 1 through 11 are numbered. Wild-type allele, targeting vector and targeted allele ($Fbln4^{neo\text{-}loxP}$, $Fbln4^{loxP}$, $Fbln4^{floxed}$) are shown. *FLPe*-mediated excision removes the neo cassette to generate the $Fbln4^{loxP}$ allele and *Cre*-mediated excision deletes exons 1-3 and generates the floxed allele ($Fbln4^{floxed}$). $Fbln4^{GKO}$ is obtained by deleting *Fbln4* in germ cells. Double-headed arrow indicates 1 kb. **B.** Southern blot analysis of ES cells. *Sac*I-digested genomic DNA hybridized with a 5' probe (shown in A) yields 11.3-kb and 8.3-kb bands for the wild-type and $Fbln4^{neo\text{-}loxP}$ alleles, respectively. XbaI-digested DNA hybridized with a 3' probe yields 10.2-kb and 3.7-kb bands for the wild-type and $Fbln4^{neo\text{-}loxP}$ alleles, respectively. **C.** Confirmation of mutant alleles by genomic PCR. Amplification with primer set 1 distinguishes the $Fbln4^{loxP}$ allele from wild-type allele. Primer set 2 only amplifies the $Fbln4^{floxd}$ allele. **D.** Ascending aortic aneurysm in E18.5 $Fbln4^{GKO}$ embryo (arrow). Tortuous descending thoracic aorta is seen in the mutant (arrowhead). **E.** Validation of the absence of *Fbln4* transcripts by qPCR. Aortae harvested from E18.5 wild-type and $Fbln4^{GKO}$ (n=6 per genotype) were analyzed. *Fbln4* expression was not detected in the $Fbln4^{GKO}$ aortae. Data are shown as means ± SD.

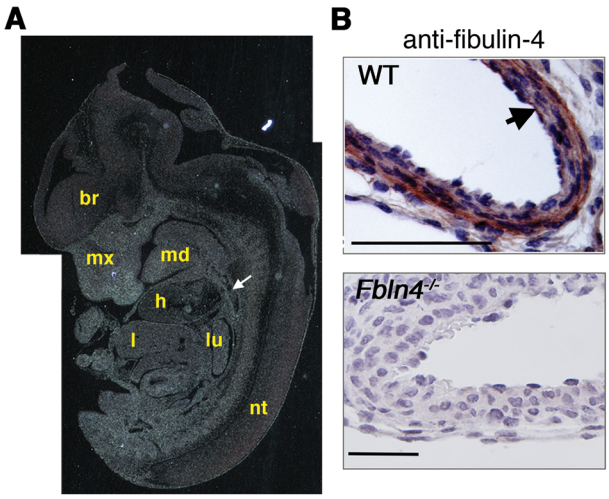

Online Figure II. A. Detection of *Fbln4* transcripts by in situ hybridization. *Fbln4* is ubiquitously expressed in the E12.0 mouse embryo. Arrow indicates the wall of developing dorsal aorta. No expression was detected in the brain (br) or neural tube (nt). md, mandibular component of the first branchial arch; mx, maxillar component of the first branchial arch; h, heart; l, liver; lu, lung. Bars indicate 200 μm. **B.** Fibulin-4 immunostaining of the aortic wall of the near-term embryo. Fibulin-4 immunoreactivity is detected in endothelial cells (arrow) and smooth muscle cells in wild-type (WT). Fibulin-4 is absent in the *Fbln4*-null vessel. Bars indicate 50 μm.

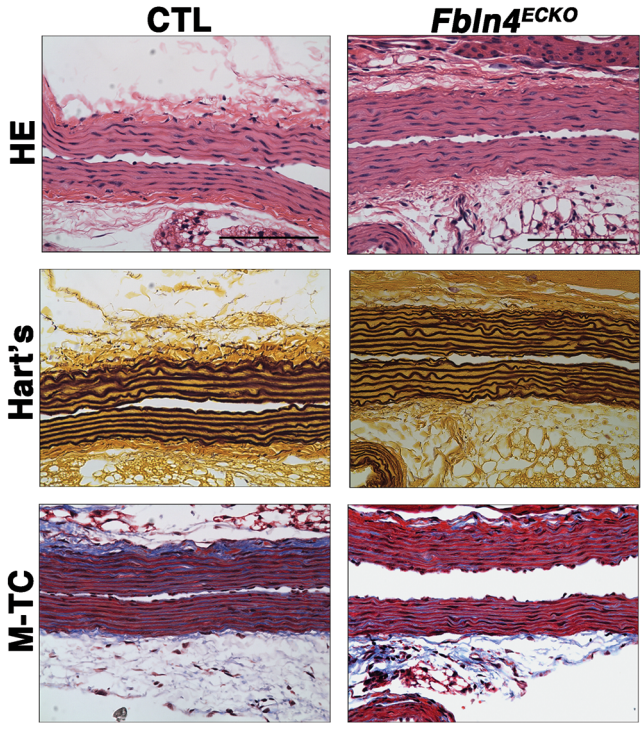

Online Figure III. Histological analysis of P90 ascending aorta from EC-specific knockout of *Fbln4* (*Fbln4*^{ECKO}). Transverse sections of control and mutant aortae were stained with HE, Hart's and Masson-Trichrome. No appreciable difference was observed between control and mutant aortae. Bars indicate 100 μm.

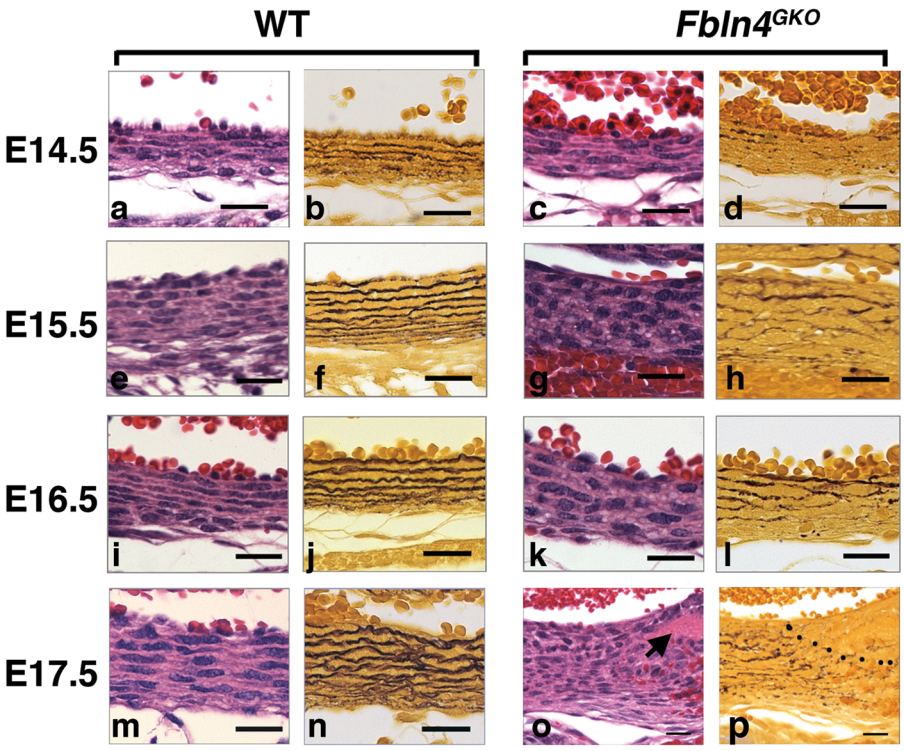

Online Figure IV. Developmental analysis of ascending aortae in *Fbln4*^{GKO} embryos. HE and Hart's staining of transverse sections of the ascending aorta from wild-type (a, b, e, f, i, j, m, n) and *Fbln4*^{GKO} (c, d, g, h, k, l, o, p) embryos at indicated time points. Hart's staining for elastic fibers shows that these structures are less formed in *Fbln4*^{GKO} embryos at all stages. At E14.5, morphology of SMCs is indistinguishable between wild-type and *Fbln4*^{GKO} (compare a and c). At E15.5, nuclei of *Fbln4*^{GKO} SMCs are round and the cells display an immature phenotype (g) and disarray of SMCs is evident by E16.5 (compare i and k). At E17.5, proliferation of SMCs and hyaline degeneration (arrow in o) are observed in the *Fbln4*^{GKO} aorta. Elastic fibers are not detected in the degenerative area (p). Bars indicate 20 μm.

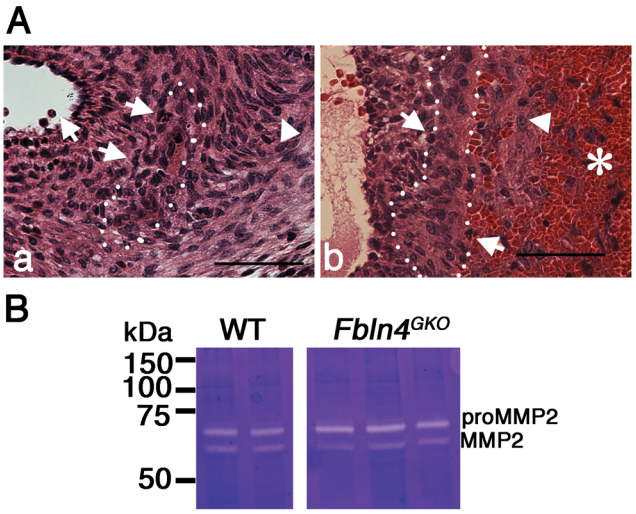

Online Figure V. Characterization of aneurysm lesions in *Fbln4*^{GKO} aorta. **A.** (a) HE staining of a small degenerative region within the medial wall (dotted area). Mild infiltration of neutrophils (arrows) and mononuclear cells (arrowhead) are seen. (b) HE staining of the aneurysm with dissection. Large area of medial wall degeneration (dotted area) and false lumen (asterisk) are shown. Bars indicate 50 μm. **B.** Representative gelatin zymogram of descending aortae from wild-type (n=4) and *Fbln4*^{GKO} (n=4) embryos at E18.5. Levels of pro-MMP2 and MMP2 are comparable between genotypes.

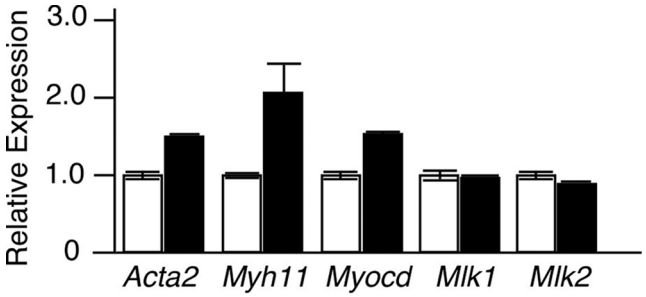

Online Figure VI. Representative qPCR analysis of SMC-specific genes in the descending thoracic aortae of P1 wild-type (white column) and *Eln*$^{-/-}$ (black column) mice. Seven aortae per genotype were pooled and subjected to qPCR. Expressions of *Acta2*, *Mhy11* and *Myocd* were increased in *Eln*$^{-/-}$ aortae. Bars indicate means ± SD.

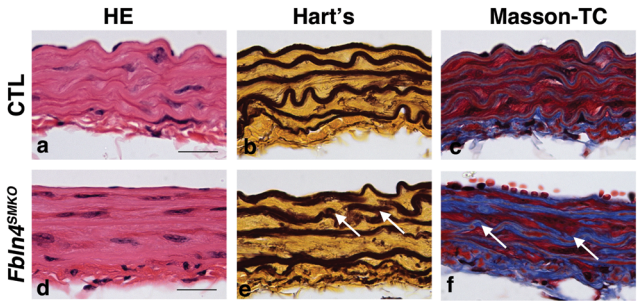

Online Figure VII. Histological analysis of P90 descending thoracic aorta from control and *Fbln4*^{SMKO} mice. Wall thickness is comparable between the control (a) and mutant aorta (d). Note relatively well-maintained elastic laminae in the mutant (compare b and e), although some discontinuities of elastic fibers were seen (arrows in e). Collagen fibers were increased in the mutant (arrows in f). Bars indicate 20 μm.

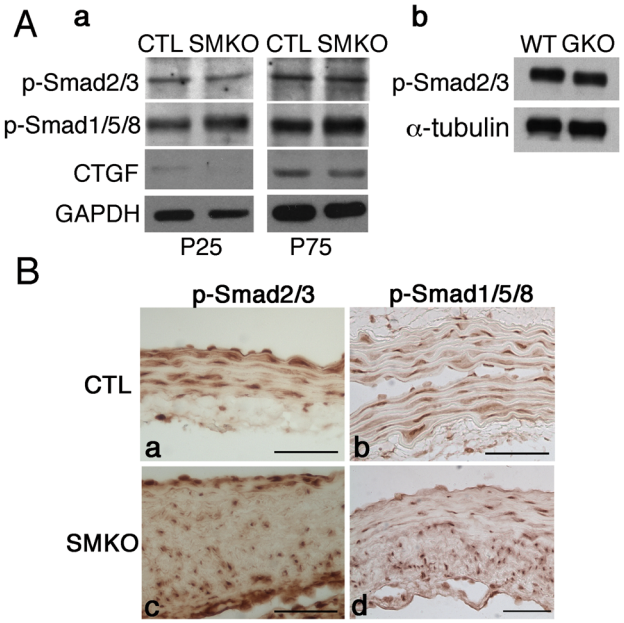

Online Figure VIII. A. a. Representative Western blots of the ascending aorta from control and *Fbln4*^{SMKO} mice at P25 and P75. P-Smad2/3 and p-Smad1/5/8 levels were comparable between control and mutant aortae. The experiments were done 3-5 times using different sibling pairs. **b.** Representative Western blots of E18.5 descending thoracic aorta from wild-type (n=3) and *Fbln4*^{GKO} (n=3) embryos. No difference was observed in p-Smad2/3 levels between wild-type and *Fbln4*^{GKO} embryos. **B.** Representative immunostaining of the P90 aorta with anti-p-Smad2/3 (a, c) and p-Smad1/5/8 (b, d) antibodies. No significant difference was observed between control and *Fbln4*^{SMKO} aortae.

Supplemental Figures and Figure leneds

Online Figure I. Generation of *Fbln4* conditional knockout mice. **A.** Targeting strategy. Exons 1 through 11 are numbered. Wild-type allele, targeting vector and targeted allele ($Fbln4^{neo\text{-}loxP}$, $Fbln4^{loxP}$, $Fbln4^{floxed}$) are shown. *FLPe*-mediated excision removes the neo cassette to generate the $Fbln4^{loxP}$ allele and *Cre*-mediated excision deletes exons 1-3 and generates the floxed allele ($Fbln4^{floxed}$). $Fbln4^{GKO}$ is obtained by deleting *Fbln4* in germ cells. Double-headed arrow indicates 1 kb. **B.** Southern blot analysis of ES cells. *Sac*I-digested genomic DNA hybridized with a 5' probe (shown in A) yields 11.3-kb and 8.3-kb bands for the wild-type and $Fbln4^{neo\text{-}loxP}$alleles, respectively. XbaI-digested DNA hybridized with a 3' probe yields 10.2-kb and 3.7-kb bands for the wild-type and $Fbln4^{neo\text{-}loxP}$ alleles, respectively. **C.** Confirmation of mutant alleles by genomic PCR. Amplification with primer set 1 distinguishes the $Fbln4^{loxP}$ allele from wild-type allele. Primer set 2 only amplifies the $Fbln4^{floxd}$ allele. **D.** Ascending aortic aneurysm in E18.5 $Fbln4^{GKO}$ embryo (arrow). Tortuous descending thoracic aorta is seen in the mutant (arrowhead). **E.** Validation of the absence of *Fbln4* transcripts by qPCR. Aortae harvested from E18.5 wild-type and $Fbln4^{GKO}$ (n=6 per genotype) were analyzed. *Fbln4* expression was not detected in the $Fbln4^{GKO}$ aortae. Data are shown as means ± SD.

Online Figure II. A. Detection of *Fbln4* transcripts by in situ hybridization. *Fbln4* is ubiquitously expressed in the E12.0 mouse embryo. Arrow indicates the wall of developing dorsal aorta. No expression was detected in the brain (br) or neural tube (nt). md, mandibular component of the first branchial arch; mx, maxillar component of the first branchial arch; h, heart; l, liver; lu, lung. Bars indicate 200 μm. **B.** Fibulin-4 immunostaining of the aortic wall of the near-term embryo. Fibulin-4 immunoreactivity is detected in endothelial cells (arrow) and smooth muscle cells in wild-type (WT). Fibulin-4 is absent in the *Fbln4*-null vessel. Bars indicate 50 μm.

Online Figure III. Histological analysis of P90 ascending aorta from EC-specific knockout of *Fbln4* ($Fbln4^{ECKO}$). Transverse sections of control and mutant aortae were stained with HE, Hart's and Masson-Trichrome. No appreciable difference was observed between control and mutant aortae. Bars indicate 100 μm.

Online Figure IV. Developmental analysis of ascending aortae in $Fbln4^{GKO}$ embryos. HE and Hart's staining of transverse sections of the ascending aorta from wild-type (a, b, e, f, i, j, m, n) and $Fbln4^{GKO}$ (c, d, g, h, k, l, o, p) embryos at indicated time points. Hart's staining for elastic fibers shows that these structures are less formed in $Fbln4^{GKO}$ embryos at all stages. At E14.5, morphology of SMCs is indistinguishable between wild-type and $Fbln4^{GKO}$ (compare a and c). At E15.5, nuclei of $Fbln4^{GKO}$ SMCs are round and the cells display an immature phenotype (g) and disarray of SMCs is evident by E16.5 (compare i and k). At E17.5, proliferation of SMCs and hyaline degeneration (arrow in o) are observed in the $Fbln4^{GKO}$ aorta. Elastic fibers are not detected in the degenerative area (p). Bars indicate 20 μm.

Online Figure V. Characterization of aneurysm lesions in $Fbln4^{GKO}$ aorta. **A.** (a) HE staining of a small degenerative region within the medial wall (dotted area). Mild infiltration of neutrophils (arrows) and mononuclear cells (arrowhead) are seen. (b) HE staining of the aneurysm with dissection. Large area of medial wall degeneration (dotted area) and false lumen (asterisk) are shown. Bars indicate 50 μm. **B.** Representative gelatin zymogram of descending aortae from wild-type (n=4) and $Fbln4^{GKO}$ (n=4) embryos at E18.5. Levels of pro-MMP2 and MMP2 are comparable between genotypes.

Online Figure VI. Representative qPCR analysis of SMC-specific genes in the descending thoracic aortae of P1 wild-type (white column) and $Eln^{-/-}$ (black column) mice. Seven aortae per genotype were pooled and subjected to qPCR. Expressions of *Acta2*, *Mhy11* and *Myocd* were increased in $Eln^{-/-}$ aortae. Bars indicate means ± SD.

Online Figure VII. Histological analysis of P90 descending thoracic aorta from control and *Fbln4*^{SMKO} mice. Wall thickness is comparable between the control (a) and mutant aorta (d). Note relatively well-maintained elastic laminae in the mutant (compare b and e), although some discontinuities of elastic fibers were seen (arrows in e). Collagen fibers were increased in the mutant (arrows in f). Bars indicate 20 μm.

Online Figure VIII. A. a. Representative Western blots of the ascending aorta from control and *Fbln4*^{SMKO} mice at P25 and P75. P-Smad2/3 and p-Smad1/5/8 levels were comparable between control and mutant aortae. The experiments were done 3-5 times using different sibling pairs. **b.** Representative Western blots of E18.5 descending thoracic aorta from wild-type (n=3) and *Fbln4*^{GKO} (n=3) embryos. No difference was observed in p-Smad2/3 levels between wild-type and *Fbln4*^{GKO} embryos. **B.** Representative immunostaining of the P90 aorta with anti-p-Smad2/3 (a, c) and p-Smad1/5/8 (b, d) antibodies. No significant difference was observed between control and *Fbln4*^{SMKO} aortae.

Supplemental Table 1. Antibodies used in this study

(1) Western blot analysis

Antibody	Dilution	Source
SM-MHC	1:3000	Biomedical Technologies, Inc.
SM α-actin	1:5000	Sigma
p-MEK1/2	1:1000	Cell Signaling
p-ERK1/2	1:1000	Cell Signaling
t-ERK	1:1000	Cell Signaling
p-JNK	1:1000	Cell Signaling
p-p38	1:1000	Cell Signaling
p-Smad2/3	1:1000	Cell Signaling
p-Smad1/5/8	1:1000	Cell Signaling
GAPDH	1:3000	Cell Signaling
α-tubulin	1:3000	Santa Cruz Biotechnology

(2) Immunostaining

Antibody	Dilution	Source
SM-MHC	1:200	Biomedical Technologies, Inc.
SM α-actin	1:200	Sigma
SMemb	1:500	Covance
p-ERK1/2	1:100	Cell Signaling
GRP78	1:100	Cell Signaling
p-Smad2/3	1:100	Cell Signaling
p-Smad1/5/8	1:100	Cell Signaling
Fibulin-4	1:100	In-house production
CD31	1:100	Pharmingen
p-Histone H3	1:100	Upstate
Alexa-488 phalloidin	1:200	Invitrogen
p-P38	1:100	Cell Signaling

Supplemental Table 2. Real-time PCR primer sequences

Gene	Forward primer (5' to 3')	Reverse primer (5' to 3')
Acta2	ATCGTCCACCGCAAATGC	AAGGAACTGGAGGCGCTG
Cnn1	AACTTCATGGATGGCCTCAAA	ACCCGGCTGCAGCTTGT
Mlck	AGAAGTCAAGGAGGTAAAGAATGATGT	CGGGTCGCTTTTCATTGC
Myh11	TCAACGCCAACCGCAGGAAGCTG	TGCTAAGCAGTCTGCTGGGCT
SM22	GCGCCTGGGCTTCCA	CAGGCTGTTCACCAATTTGCT
Myocd	CACCCCACGACATCAAATCC	TGCATCATTCTTGTCACTTTCTGA
Mkl1	TCCACTTAGTGAGCGGAAGAA	CCTTGGCTCACCAGTTCCT
Mkl2	ACCTCCTGTGACTGCAAGCA	GGGTTTTCAAGAATTCAGGAACTG
Srf	GTCTCCCTCTCGTGACAGCAG	CAGTTGTGGGTACAGACGACGT
Fbln4	GCA CTG CCG GGA TGT CA	GCA TTT CAT CTC ACC CTT GCA
B2m	CCGAGCCCAAGACCGTCTA	AACTGGATTTGTAATTAAGCAGGTTCA

Supplemental References

1. McLaughlin PJ, Chen Q, Horiguchi M, Starcher BC, Stanton JB, Broekelmann TJ, Marmorstein AD, McKay B, Mecham R, Nakamura T, Marmorstein LY. Targeted disruption of fibulin-4 abolishes elastogenesis and causes perinatal lethality in mice. *Mol Cell Biol.* 2006;26:1700-1709.
2. Li DY, Brooke B, Davis EC, Mecham RP, Sorensen LK, Boak BB, Eichwald E, Keating MT. Elastin is an essential determinant of arterial morphogenesis. *Nature.* 1998;393:276-280.
3. Sakai K, Miyazaki J. A transgenic mouse line that retains Cre recombinase activity in mature oocytes irrespective of the cre transgene transmission. *Biochem Biophys Res Commun.* 1997;237:318-324.
4. Kisanuki YY, Hammer RE, Miyazaki J, Williams SC, Richardson JA, Yanagisawa M. Tie2-Cre transgenic mice: a new model for endothelial cell-lineage analysis in vivo. *Dev Biol.* 2001;230:230-242.
5. Yanagisawa H, Yanagisawa M, Kapur RP, Richardson JA, Williams SC, Clouthier DE, de Wit D, Emoto N, Hammer RE. Dual genetic pathways of endothelin-mediated intercellular signaling revealed by targeted disruption of endothelin converting enzyme-1 gene. *Development.* 1998;125:825-836.
6. Rodriguez CI, Buchholz F, Galloway J, Sequerra R, Kasper J, Ayala R, Stewart AF, Dymecki SM. High-efficiency deleter mice show that FLPe is an alternative to Cre-loxP. *Nat Genet.* 2000;25:139-140.
7. Yanagisawa H, Richardson JA, Taurog JD, Hammer RE. Characterization of psoriasiform and alopecic skin lesions in HLA-B27 transgenic rats. *Am J Pathol.* 1995;147:955-964.
8. Davis EC. Smooth muscle cell to elastic lamina connections in developing mouse aorta. Role in aortic medial organization. *Lab Invest.* 1993;68:89-99.
9. Spencer JA, Hacker SL, Davis EC, Mecham RP, Knutsen RH, Li DY, Gerard RD, Richardson JA, Olson EN, Yanagisawa H. Altered vascular remodeling in fibulin-5-deficient mice reveals a role of fibulin-5 in smooth muscle cell proliferation and migration. *Proc Natl Acad Sci U S A.* 2005;102:2946-2951.